

Dimension six FCNC operators and top production at the LHC

R.A. Coimbra^{1,2 *}, P.M. Ferreira^{3,4 †}, R.B. Guedes^{4 ‡}, O.

Oliveira^{2 §}, A. Onofre^{1 ¶}, R. Santos^{5 **} and Miguel Won^{1,5 ††}

¹ *LIP- Departamento de Física, Universidade de Coimbra, 3004-516 Coimbra, Portugal;*

² *Centro de Física Computacional, Universidade de Coimbra, 3004-516 Coimbra, Portugal;*

³ *Instituto Superior de Engenharia de Lisboa,*

Rua Conselheiro Emídio Navarro 1, 1959-007 Lisboa, Portugal;

⁴ *Centro de Física Teórica e Computacional,*

Faculdade de Ciências, Universidade de Lisboa,

Avenida Professor Gama Pinto, 2, 1649-003 Lisboa, Portugal;

⁵ *NExT Institute and School of Physics and Astronomy,*

University of Southampton Highfield, Southampton SO17 1BJ, United Kingdom

(Dated: January 6, 2009)

In this work we calculate the effects of the electroweak flavour changing neutral currents dimension six effective operators on single top production at the LHC. These results are then combined with previous ones we have obtained for the strong sector. This allow us, for the first time, to perform a combined analysis of flavour changing neutral currents in top production with all contributing dimension six operators. Finally, we study the feasibility of their observation and characterization both at the Tevatron and at the LHC.

I. INTRODUCTION

CERN's Large Hadron Collider (LHC) will soon start colliding protons with 14 TeV center of mass energy. This top quark factory will allow us to study the least known of all quarks with unprecedented precision. The study of flavour changing neutral currents (FCNC) is one of the most interesting research topics related to top quark physics as a wide variety of models shows a strong dependence in the measurable FCNC quantities. In fact, the top quark FCNC branching ratios can vary from extremely small in the Standard Model (SM) to measurable values at the LHC in some of its extensions.

In a series of papers [1, 2, 3, 4] we studied flavour changing single top production using the effective operator formalism [5]. In [1, 2, 3] we assumed that new physics would originate from strong interactions alone. Consequently, we have calculated the FCNC top decay branching ratio $t \rightarrow u(c)g$ as well as all cross sections for single top production using the new dimension six operators stemming from the strong sector. These production processes included associated production of a single top quark alongside a jet, a Higgs boson or an electroweak gauge boson. The main conclusion was that for large values of $\text{BR}(t \rightarrow qg)$, with $q = u, c$, these processes might be observable at the LHC.

Not all of the processes calculated for the LHC receive contributions from new strong interactions alone - some processes are also modified by dimension six operators from the electroweak sector, that is, by operators that do not include the strong field tensor. In a recent paper [4] we have investigated the possibility of distinguishing the contributions from the strong and from the electroweak sectors for the FCNC processes $pp \rightarrow tZ$ and $pp \rightarrow t\gamma$. We found new physical relations between cross sections, branching ratios and coupling constants from both sectors. More importantly we showed that the electroweak and the strong sectors could be distinguished in a large portion of the parameter space. We also showed that the interference between both FCNC sectors is mostly constructive. It is also worth mentioning that a near-proportionality between the cross section of associated top plus photon

* rita@teor.fis.uc.pt

† ferreira@cii.fc.ul.pt

‡ renato@ci.fc.ul.pt

§ orlando@teor.fis.uc.pt

¶ onofre@lipc.fis.uc.pt

** rsantos@cii.fc.ul.pt

†† miguel.won@lipc.fis.uc.pt

production at the LHC and the sum of the FCNC decays of the top to a photon and a gluon was found. Finally, we have estimated the backgrounds to these processes and concluded that one might expect a significant number of events at the LHC.

In this work we plan to extend this study to the electroweak FCNC contributions to processes $pp \rightarrow t\bar{q}(q\bar{q} \rightarrow t\bar{q})$, $pp \rightarrow tq(qq \rightarrow tq)$ and complex conjugate processes and $pp \rightarrow t\bar{t}$. This will finally put us in a position to discuss FCNC single top production and decay with all the contributions from new physics considered taken into account. Before going any further let us stress that the choice of operators followed a very simple rule: it had to contain one and only one top quark and at least one gauge boson. Therefore, these operators will always give rise to FCNC vertices contributing to the top quark FCNC decays to a light quark and a neutral gauge boson, either strong or electroweak. These operators have only to obey our selection criteria to be explained in detail later - not to affect low energy physics. How far can one go in distinguishing the different sectors and if possible even the different operators of the theory? This is what we are pursuing in this work - probing the actual models proposed in the literature, and perhaps new ones, is the ultimate goal of this entire project.

There is a guiding principle in our choice of operators in all analysis done so far. We choose the dimension six operators that have no sizeable impact on low energy physics. B physics [6] is the main source of constraints, due to the gauge structure of the SM. Empirically, we expect a hierarchy of constraints resulting from the underlying SM gauge structure. Therefore, the operators denoted by *LL* which are the ones built with two *SU(2)* doublets are those where the gauge structure is felt more strongly. On the contrary, *RR* operators should be the least constrained, as there is no relation between a *R* top quark and *R* bottom quark. A recent study based on constraints from B physics [6] has proven our criteria to be well established. Using the LHC [7, 8, 9] predictions they were able to show that, in fact, some of the constraints on dimension 6 operators stemming from low energy physics are already stronger than what is predicted that could be measured at the LHC. The expected bounds obtained for a luminosity of 100 fb^{-1} are below the limits obtained for the *LL* operators. As expected, they conclude that the *RR* operators will definitely be probed at the LHC, while limits on *LR* and *RL* operators are close to those experimental bounds. Finally, we note that the Tevatron and the B factories are still collecting data. Therefore the constraints will be even stronger by the time the LHC starts to analyse data. However, it should be noted that that are models where cancellations between different operators of type *LL* could occur [10]. Those models could avoid B physics bounds and have definitely to be analyzed in more detail regarding the constraints from B physics.

The use of anomalous couplings to study possible new top physics at the LHC and Tevatron has been the subject of many works [11]. We just highlight here what are the main advantages of our approach: first of all, it is the first time that a calculation with a complete set of operators from both the strong and electroweak sectors is made for single top production involving FCNC. Whenever possible and relevant, we have presented all the expressions for the cross sections and branching ratios allowing the use by others and in particular in the generators available in the market. In the papers published so far we have tried to put the emphasis on the relation between the physical quantities, avoiding as much as possible the use of the coupling constants related to each particular operator. When doing so one has to keep in mind that the dependence in the coupling constants is however still there and has to be handled with care. Finally we note that contrary to the form factor approach, the use of the effective operator formalism has predictive power - the underlying gauge structure reflects itself in relations between the several physical quantities. We will use all available experimental data available to restrict the parameter space. In particular we will use the most recent data on single top production by the CDF [12] and D0 [13] collaborations as well as the data on the direct FCNC top production published by CDF [14].

This paper is organised as follows: in section II we review the effective operator formalism and introduce our FCNC operators, explaining what physical criteria were behind their choice. In section III we use those same Feynman rules to compute and analyse the branching ratios of the top quark FCNC decays. In the following two sections we study the cross sections for production of a single top with all FCNC interactions - both strong and electroweak - included. In section V we present the integrated cross section results predicted for the Tevatron and the LHC, and discuss the impact our FCNC operators will have on observables such as the cross section for top + jet production. Finally, we will draw general conclusions in section VI.

II. FLAVOUR CHANGING EFFECTIVE OPERATORS

The effective operator formalism of Buchmüller and Wyler [5] is based on the assumption that far below some characteristic scale Λ the world is well-described by the Standard Model of particle physics. Any new physical effects not yet observed can be accounted for with the introduction of an effective Lagrangian with a set of new interactions to be determined phenomenologically. Such a Lagrangian would be valid at very high energies but, at a lower energy scale, we would only perceive its effects through a set of effective operators of dimensions higher than four. The form of the effective Lagrangian is independent of the model from which it is derived and the new effective operators are only constrained by the symmetries of low energy physics, that is, those of the SM. This is why the effective Lagrangian approach is ideally suited for studying possible effects of physics beyond the SM. The effective lagrangian can be written as a series in the energy scale, such that

$$\mathcal{L} = \mathcal{L}^{SM} + \frac{1}{\Lambda} \mathcal{L}^{(5)} + \frac{1}{\Lambda^2} \mathcal{L}^{(6)} + O\left(\frac{1}{\Lambda^3}\right) , \quad (1)$$

where \mathcal{L}^{SM} is the SM lagrangian and $\mathcal{L}^{(5)}$ and $\mathcal{L}^{(6)}$ contain all the dimension five and six operators which, like \mathcal{L}^{SM} , are invariant under the gauge symmetries of the SM. The number of effective operators is obviously infinite which means that the expansion has to be truncated at some point. We will be working at the TeV scale (2 TeV for the Tevatron and 14 TeV for the LHC) and therefore we choose to discard operators of dimension higher than six, as terms of order equal or superior to $1/\Lambda^3$ ought to be quite small, and not contribute to TeV-scale physics. The dimension five terms in the Lagrangian will not be considered in our analysis as they break baryon and lepton number conservation. The list of dimension six operators is quite vast and can be found in [5].

A. Effective operators in the strong sector

In [1, 3] we have studied all flavour changing effective operators with one top quark, some other quark and which included a gluonic field tensor. We have named them strong effective FCNC operators as they would change the strong interactions. We remind that our criteria in choosing these operators were that they contributed only to FCNC top physics, not affecting low energy physics. In that sense, operators that contributed to top quark phenomenology but which also affected bottom quark physics (in the notation of ref. [5], operators \mathcal{O}_{qG}) were not considered. In accordance with our criteria there are only two dimension six operators in the strong sector that can generate interactions with two fermions and one gluon. Following the notation of [5] we write these operators as

$$\mathcal{O}_{tG\phi} = \frac{\beta_{it}^S}{\Lambda^2} (\bar{q}_L^i \lambda^a \sigma^{\mu\nu} t_R) \tilde{\phi} G^{a\mu\nu} , \quad (2)$$

and

$$\mathcal{O}_{tG} = i \frac{\alpha_{it}^S}{\Lambda^2} \bar{u}_R^i \lambda^a \gamma_\mu D_\nu t_R G^{a\mu\nu} , \quad (3)$$

where the coefficients α_{it}^S and β_{it}^S are complex dimensionless couplings. $G_{\mu\nu}^a$ is the gluonic field tensor, u_R^i stands for a right-handed quark singlet and q_L^i represents the left-handed quark. FCNC occurs because these fields belong to the first and second generation. There are also operators, with couplings α_{ti}^S and β_{ti}^S , where the positions of the top and u , q^i spinors are exchanged in the expressions above. The hermitian conjugate of all operators are obviously included in the lagrangian. These operators will originate FCNC vertices of the form $g t \bar{u}_i$ (with $u_i = u, c$). Due to covariant derivative acting on a quark spinor, the operators with α^S couplings also contribute to quartic vertices of the form $g g t \bar{u}_i$, $g \gamma t \bar{u}_i$ and $g Z t \bar{u}_i$.

B. Effective operators in the electroweak sector

In this section we present the operators stemming from the electroweak sector that would give rise to new FCNC interactions involving the top quark. They would in particular contribute to the FCNC top

decays $t \rightarrow q Z$ and $t \rightarrow q \gamma$, where $q = u, c$. First we consider the chirality flipping operators that in a renormalizable theory are present only at one-loop level. They are equivalent to the ones in the strong sector, the only difference being the gluonic tensor replaced by the U(1) and SU(2) field tensors. They can be written as

$$\begin{aligned} \mathcal{O}_{tB} &= i \frac{\alpha_{it}^B}{\Lambda^2} \bar{u}_R^i \gamma_\mu D_\nu t_R B^{\mu\nu} , \\ \mathcal{O}_{tB\phi} &= \frac{\beta_{it}^B}{\Lambda^2} (\bar{q}_L^i \sigma^{\mu\nu} t_R) \tilde{\phi} B_{\mu\nu} , \quad \mathcal{O}_{tW\phi} = \frac{\beta_{it}^W}{\Lambda^2} (\bar{q}_L^i \tau_I \sigma^{\mu\nu} t_R) \tilde{\phi} W_{\mu\nu}^I , \end{aligned} \quad (4)$$

where $B^{\mu\nu}$ and $W_{\mu\nu}^I$ are the $U(1)_Y$ and $SU(2)_L$ field tensors. The couplings $\alpha_{ti}^B, \beta_{ti}^B$ and β_{ti}^W are complex dimensionless couplings (the couplings corresponding to the exchange of quark spinors, and the hermitian conjugates of the operators above, were also considered).

Expanding these operators and diagonalizing the fields' mass matrices we obtain the terms of the form $Z \bar{t} u_i$ and $\gamma \bar{t} u_i$. The operators considered here give no contribution to both the gauge boson and the fermions mass matrices. This allows us to write these operators with the fermion mass eigenstates from the start with no loss of generality. For the same reason, the relation between the gauge bosons mass eigenstates and group eigenstates is the same as in the SM, i.e., they are still related through the well-known Weinberg rotation. New effective couplings $\{\alpha^\gamma, \beta^\gamma\}$ and $\{\alpha^Z, \beta^Z\}$, related to the initial couplings via the Weinberg angle θ_W , are given by

$$\alpha^\gamma = \cos \theta_W \alpha^B \quad , \quad \alpha^Z = -\sin \theta_W \alpha^B \quad (5)$$

and

$$\begin{cases} \beta^\gamma = \sin \theta_W \beta^W + \cos \theta_W \beta^B \\ \beta^Z = \cos \theta_W \beta^W - \sin \theta_W \beta^B \end{cases} . \quad (6)$$

We showed in [4] that the Weinberg rotation introduces a certain correlation between FCNC processes involving the photon or the Z , barring some bizarre and unnatural cancellation between anomalous couplings in eq. (6).

Besides chirality-flipping operators there are chirality conserving operators. These are tree-level operators in the sense that their flavour conserving versions are already present in the SM at tree-level. In fact, if we consider the vertex $\bar{t}tZ$, we see that it has two vector contributions of different magnitudes, one proportional to $\gamma_\mu \gamma_L$ and the other proportional to $\gamma_\mu \gamma_R$. The anomalous operators would then contribute to modify the Z boson neutral current. The Higgs field has no electric charge but still interacts with the Z boson. Thus, there extra effective operators which contribute to Z FCNC interactions, analogous to those considered in [15] to study FCNC in the leptonic sector. They are given by

$$\mathcal{O}_{D_t} = \frac{\eta_{it}}{\Lambda^2} (\bar{q}_L^i D^\mu t_R) D_\mu \tilde{\phi} , \quad \mathcal{O}_{\bar{D}_t} = \frac{\bar{\eta}_{it}}{\Lambda^2} (D^\mu \bar{q}_L^i t_R) D_\mu \tilde{\phi} \quad (7)$$

and

$$\mathcal{O}_{\phi_t} = \theta_{it} (\phi^\dagger D_\mu \phi) (u_R^i \gamma^\mu t_R) , \quad (8)$$

and another operator with coupling θ_{ti} with the position of the u^i and t spinors exchanged. As before, the coefficients $\eta_{it}, \bar{\eta}_{it}$ and θ_{it} are complex dimensionless couplings. For simplicity we redefine the η and θ couplings as $\eta \rightarrow (\sin(2\theta_W)/e) \eta$ and $\theta \rightarrow (\sin(2\theta_W)/e) (\theta_{it} - \theta_{ti}^*)$. The Feynman rules for the FCNC triple vertices are shown in the appendix. Just like for the anomalous operators in the strong sector, the gauge structure of the terms in the electroweak lagrangian gives rise to new quartic vertices. We will not need those vertices in this work and refer the reader to [4] for details.

III. FCNC BRANCHING RATIOS OF THE TOP

In the SM the top decays to a light quark and a neutral gauge boson only at the loop-level. This fact, together with the Glashow-Iliopoulos-Maiani (GIM) mechanism, is the reason for the immense

suppression of the branching ratios of these rare top decays in the SM. They can however be much larger in extensions of the SM. If new particles are present, the GIM mechanism can be avoided and, with the addition of potentially large coupling constants from the new interactions, the branching ratios can be enhanced by as much as thirteen orders of magnitude. For instance, in the SM the branching ratio for the decay $t \rightarrow u Z$ is of the order of $\sim 10^{-16}$, whereas in a quark-singlet model it can reach values of as much as 10^{-4} . For supersymmetry or two Higgs double models, the top quark FCNC branching ratios are typically of the order of 10^{-6} - 10^{-4} . For more details see [16, 17].

The effective operator formalism allows us to describe, in a model-independent manner, the possible rare decays of the top. In ref. [1] we computed the branching ratios for the FCNC top decays $t \rightarrow q g$, due to the strong sector anomalous operators therein introduced. The decay width for $t \rightarrow u g$ is given by

$$\Gamma(t \rightarrow ug) = \frac{m_t^3}{12\pi\Lambda^4} \left\{ m_t^2 |\alpha_{tu}^S + (\alpha_{ut}^S)^*|^2 + 16v^2 (|\beta_{tu}^S|^2 + |\beta_{ut}^S|^2) + 8v m_t \text{Im} [(\alpha_{ut}^S + (\alpha_{tu}^S)^*) \beta_{tu}^S] \right\}, \quad (9)$$

with an analogous expression for $\Gamma(t \rightarrow cg)$, with different couplings. In ref. [4] we have repeated the calculation for the electroweak sector new FCNC decays, namely, $t \rightarrow u\gamma$ (and $t \rightarrow c\gamma$, with *a priori* different couplings), for which we have obtained a width given by the following expression

$$\Gamma(t \rightarrow u\gamma) = \frac{m_t^3}{64\pi\Lambda^4} \left\{ m_t^2 |\alpha_{tu}^\gamma + (\alpha_{ut}^\gamma)^*|^2 + 16v^2 (|\beta_{tu}^\gamma|^2 + |\beta_{ut}^\gamma|^2) + 8v m_t \text{Im} [(\alpha_{ut}^\gamma + (\alpha_{tu}^\gamma)^*) \beta_{tu}^\gamma] \right\}. \quad (10)$$

Notice how similar this result is to eq. (9). We will also have contributions [4] from these operators to $t \rightarrow uZ$ ($t \rightarrow cZ$), from which we obtain a width given by

$$\begin{aligned} \Gamma(t \rightarrow uZ) = & \frac{(m_t^2 - m_Z^2)^2}{32m_t^3\pi\Lambda^4} \left[K_1 |\alpha_{ut}^Z|^2 + K_2 |\alpha_{tu}^Z|^2 + K_3 (|\beta_{ut}^Z|^2 + |\beta_{tu}^Z|^2) + K_4 (|\eta_{ut}|^2 + |\bar{\eta}_{ut}|^2) \right. \\ & + K_5 |\theta|^2 + K_6 \text{Re} [\alpha_{ut}^Z \alpha_{tu}^Z] + K_7 \text{Im} [\alpha_{ut}^Z \beta_{tu}^Z] \\ & + K_8 \text{Im} [\alpha_{tu}^{Z*} \beta_{tu}^Z] + K_9 \text{Re} [\alpha_{ut}^Z \theta^*] + K_{10} \text{Re} [\alpha_{tu}^Z \theta] \\ & \left. + K_{11} \text{Re} [\beta_{ut}^Z (\eta_{ut} - \bar{\eta}_{ut})^*] + K_{12} \text{Im} [\beta_{tu}^Z \theta] + K_{13} \text{Re} [\eta_{ut} \bar{\eta}_{ut}^*] \right], \end{aligned} \quad (11)$$

where the coefficients K_i are given by

$$\begin{aligned} K_1 &= \frac{1}{2} (m_t^4 + 4m_t^2 m_Z^2 + m_Z^4) & K_2 &= \frac{1}{2} (m_t^2 - m_Z^2)^2 & K_3 &= 4(2m_t^2 + m_Z^2)v^2 \\ K_4 &= \frac{v^2}{4m_Z^2} (m_t^2 - m_Z^2)^2 & K_5 &= \frac{v^4}{m_Z^2} (m_t^2 + 2m_Z^2) & K_6 &= (m_t^2 - m_Z^2)(m_t^2 + m_Z^2) \\ K_7 &= 4m_t(m_t^2 + 2m_Z^2)v & K_8 &= 4m_t(m_t^2 - m_Z^2)v & K_9 &= -2(2m_t^2 + m_Z^2)v^2 \\ K_{10} &= -2(m_t^2 - m_Z^2)v^2 & K_{11} &= -K_{10} & K_{12} &= -12m_t v^3 & K_{13} &= \frac{-v^2}{m_Z^2} K_2. \end{aligned} \quad (12)$$

FCNC processes were the subject of searches by several experimental groups. Indirect bounds [6, 26] are provided mostly by electroweak precision physics and B and K physics. Due to the SM gauge structure, B physics can be used to set limits on operators that involve top and bottom quarks. The strongest bounds so far are the ones in [6] where invariance under $SU(2)_L$ is required for the set of operators chosen. Regarding $Br(t \rightarrow qZ)$ and $Br(t \rightarrow q\gamma)$, the only direct bounds available to date are the ones

	LEP	HERA	Tevatron
$Br(t \rightarrow q Z)$	< 7.8% [18]	< 49% [19]	< 3.7% ^d [20]
$Br(t \rightarrow q \gamma)$	< 2.4% [18]	< 0.75% [19]	< 3.2% ^d [21]
$Br(t \rightarrow q g)$	< 17% [22]	< 13% [19, 23]	< $O(0.1 - 1\%)$ [24, 25]

TABLE I: Current experimental bounds on FCNC branching ratios. The superscript “d” refers to bounds obtained from direct measurements, as is explained in the text.

from the Tevatron (CDF). The CDF collaboration has searched its data for signatures of $t \rightarrow q \gamma$ and $t \rightarrow q Z$ (where $q = u, c$). Both analyses use $p\bar{p} \rightarrow t\bar{t}$ data and assume that one of the tops decays according to the SM into $W b$. We have collected all these experimental results in Table I. LEP and ZEUS have translated to bounds on the branching ratios, experimental limits originally obtained for the cross section. The translation is straightforward as it was done via just one operator, the chromomagnetic one. Note that LEP bounds are derived assuming the same anomalous coupling for the u and c quarks while the ZEUS bound is only for the process involving a u quark. With forthcoming Tevatron data, we expect that these bounds will improve in the near future. The same searches are being prepared for the LHC. A detailed discussion with all present bounds on FCNC and the predictions for the LHC can be found in [7, 8, 9]. With a luminosity of 100 fb^{-1} and in the absence of signal, the 95% confidence level bounds on the branching ratios give us $Br(t \rightarrow q Z) \sim 10^{-5}$, $Br(t \rightarrow q \gamma) \sim 10^{-5}$ and $Br(t \rightarrow q g) \sim 10^{-4}$.

IV. ELECTROWEAK FCNC CONTRIBUTIONS TO TOP + QUARK PRODUCTION

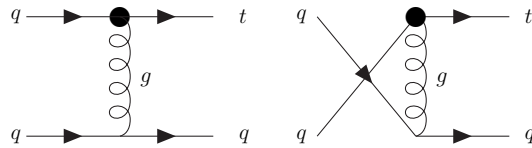
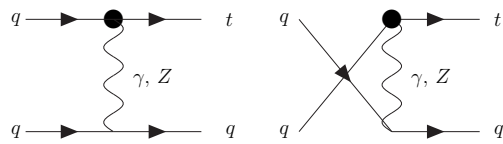
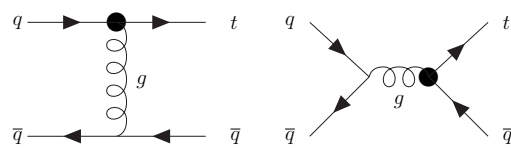
In previous references [2], we calculated the FCNC cross sections for several processes of single top production. To wit, all of the strong-FCNC contributions to the processes $pp \rightarrow qg \rightarrow gt$, $pp \rightarrow gg \rightarrow \bar{q}t$, $pp \rightarrow qq \rightarrow qt$, and respective charged conjugate processes. This amounted to a complete calculation for $pp \rightarrow t + \text{jet}$ in the strong sector. Now, in reference [4] it was shown that the electroweak FCNC interactions can have contributions to processes of associated top production alongside a neutral gauge boson as large as the strong ones. Thus, in order for us to have the complete FCNC contribution to the cross section for top + jet production, it becomes imperative to compute the electroweak FCNC contributions to this process, and their interference with the strong FCNC vertices. It is of great interest to possess a complete FCNC expression for this cross section, as it is one of the most basic top quark observables that can be measured in colliders.

Obviously, the electroweak sector will give no contribution to processes with gluons in the initial or final states. Only the processes presented in table II will be modified, which constitute all possibilities for the single top channel $qg \rightarrow tq$. The processes in table II should be divided in two groups. Processes 6 to 8 are present in the SM at tree-level while processes 1 to 5 appear only at the loop-level. The first new terms for processes 6 to 8 are therefore the interference between the SM term and the order $1/\Lambda^2$ contributions from the effective Lagrangian. For channels 1 to 5 the first term is the square of the term of order $1/\Lambda^2$ in the Lagrangian. Naively, one would expect terms 6 to 8 to be much larger than the 1 to 5 ones because of their dependence in the scale of new physics. However, due to a very strong cancellation caused by the Cabibbo-Kobayashi-Maskawa (CKM) matrix elements, it turns out that the interference between the tree-level SM processes and the anomalous ones are extremely small. Hence, contrary to what we would expect, the anomalous contributions at the lowest order in Λ are not the best ones to look for FCNC physics beyond the SM, at least in this channel. Processes 1 to 5, although of order $1/\Lambda^4$, are indeed much larger than the last ones, since in this case no CKM cancellation takes place. Finally, we remind that there are $1/\Lambda^4$ contributions to processes 6 to 8 as well. However, terms of dimension eight in the effective Lagrangian would interfere with the SM tree-level process to give terms of that same order. According to the philosophy we have adopted, we decided not to take them into account as the calculation would not be complete.

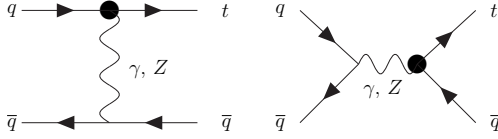
In figures (1) and (2) we show the strong and electroweak contributions, respectively, to the process $pp \rightarrow qg \rightarrow qt$. Both processes proceed through a t and a u channel. In figures (3) and (4) we show the strong and electroweak contributions, respectively, to the process $pp \rightarrow q\bar{q} \rightarrow t\bar{q}$. Note that we only consider processes where there is a “single” flavour violation, that is a single FCNC vertex per diagram. Now, in the work of refs. [1, 2, 3, 4] we endeavoured to present analytical expressions for all cross sections

Single top channel Process number	
$u u \rightarrow t u$	1
$u c \rightarrow t c$	2
$u \bar{u} \rightarrow t \bar{u}$	3
$u \bar{u} \rightarrow t \bar{c}$	4
$u \bar{c} \rightarrow t \bar{c}$	5
$d \bar{d} \rightarrow t \bar{u}$	6
$u d \rightarrow t d$	7
$u \bar{d} \rightarrow t \bar{d}$	8

TABLE II: List of single top production channels through quark-quark scattering.

FIG. 1: Feynman diagrams for strong FCNC $t q$ production.FIG. 2: Feynman diagrams for electroweak FCNC $t q$ production.FIG. 3: Feynman diagrams for strong FCNC $t \bar{q}$ production.

and decay widths computed, to make them available to whomever might wish to use them. For the full $t + q$ cross section expression, however, that is no longer practical, as the formulae are extremely lengthy. For the reader to appreciate the level of complexity of the results we obtained, suffice it to say that the

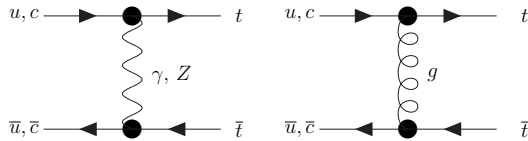
FIG. 4: Feynman diagrams for electroweak FCNC $t\bar{q}$ production.

full cross section is a sum of 66 different combinations of anomalous couplings, namely

$$\begin{aligned}
 \frac{d\sigma}{dt} = & F_1 |\alpha_{ut}^S|^2 + F_2 |\alpha_{tu}^S|^2 + F_3 [|\beta_{ut}^S|^2 + |\beta_{tu}^S|^2] + F_4 \text{Re}(\alpha_{ut}^S \alpha_{tu}^S) + F_5 \text{Im}(\alpha_{ut}^S \beta_{tu}^S) \\
 & + F_6 \text{Im}(\alpha_{tu}^S \beta_{tu}^{S*}) + G_1 |\alpha_{ut}^\gamma|^2 + G_2 |\alpha_{tu}^\gamma|^2 + G_3 [|\beta_{ut}^\gamma|^2 + |\beta_{tu}^\gamma|^2] + G_4 \text{Re}(\alpha_{ut}^\gamma \alpha_{tu}^\gamma) \\
 & + G_5 \text{Im}(\alpha_{ut}^\gamma \beta_{tu}^\gamma) + G_6 \text{Im}(\alpha_{tu}^\gamma \beta_{tu}^{\gamma*}) + H_1 |\alpha_{ut}^Z|^2 + H_2 |\alpha_{tu}^Z|^2 + H_3 |\beta_{ut}^Z|^2 \\
 & + H_4 |\beta_{tu}^Z|^2 + H_5 [|\eta|^2 + |\bar{\eta}|^2 - 2 \text{Re}(\eta \bar{\eta}^*)] + H_6 |\theta|^2 + H_7 \text{Re}(\alpha_{ut}^Z \alpha_{tu}^Z) + H_8 \text{Im}(\alpha_{ut}^Z \beta_{tu}^Z) \\
 & + H_9 \text{Re}(\alpha_{ut}^Z \theta^*) + H_{10} \text{Im}(\alpha_{tu}^Z \beta_{tu}^{Z*}) + H_{11} \text{Re}(\alpha_{tu}^Z \theta) + H_{12} [\text{Re}(\beta_{ut}^Z \eta^*) - \text{Re}(\beta_{ut}^Z \bar{\eta}^*)] \\
 & + H_{13} \text{Im}(\beta_{tu}^Z \theta) + FG_1 \text{Re}(\alpha_{ut}^S \alpha_{ut}^{\gamma*}) + FG_2 [\text{Re}(\alpha_{ut}^S \alpha_{tu}^\gamma) + \text{Re}(\alpha_{tu}^S \alpha_{ut}^\gamma) - \text{Re}(\alpha_{tu}^S \alpha_{tu}^{\gamma*})] \\
 & + FG_3 [\text{Im}(\alpha_{ut}^S \beta_{tu}^\gamma) + \text{Im}(\beta_{tu}^S \alpha_{ut}^\gamma)] + FG_4 [\text{Re}(\beta_{ut}^S \beta_{ut}^{\gamma*}) + \text{Re}(\beta_{tu}^S \beta_{tu}^{\gamma*})] \\
 & + FH_1 \text{Re}(\alpha_{ut}^S \alpha_{ut}^{Z*}) + FH_2 [\text{Re}(\alpha_{ut}^S \alpha_{tu}^Z) + \text{Re}(\alpha_{tu}^S \alpha_{ut}^Z) - \text{Re}(\alpha_{tu}^S \alpha_{tu}^{Z*})] \\
 & + FH_3 [\text{Im}(\alpha_{ut}^S \beta_{tu}^Z) + \text{Im}(\beta_{tu}^S \alpha_{ut}^Z)] + FH_4 \text{Re}(\alpha_{ut}^S \theta^*) + FH_5 \text{Re}(\alpha_{tu}^S \theta) \\
 & + FH_6 \text{Re}(\beta_{ut}^S \beta_{ut}^{Z*}) + FH_7 [\text{Re}(\beta_{ut}^S \eta^*) - \text{Re}(\beta_{ut}^S \bar{\eta}^*)] + FH_8 \text{Re}(\beta_{tu}^S \beta_{tu}^{Z*}) \\
 & + FH_9 \text{Im}(\beta_{tu}^S \theta) + GH_1 \text{Re}(\alpha_{ut}^\gamma \alpha_{ut}^Z) + GH_2 [\text{Re}(\alpha_{ut}^\gamma \alpha_{tu}^Z) + \text{Re}(\alpha_{tu}^\gamma \alpha_{ut}^Z)] \\
 & + GH_3 [\text{Im}(\alpha_{ut}^\gamma \beta_{tu}^Z) + \text{Im}(\beta_{tu}^\gamma \alpha_{ut}^Z)] + GH_4 \text{Re}(\alpha_{ut}^\gamma \theta) + GH_5 \text{Re}(\alpha_{tu}^\gamma \alpha_{tu}^{Z*}) \\
 & + GH_6 [\text{Im}(\alpha_{tu}^\gamma \beta_{tu}^{Z*}) + \text{Im}(\beta_{tu}^\gamma \alpha_{tu}^{Z*})] + GH_7 \text{Re}(\alpha_{tu}^\gamma \theta) + GH_8 \text{Re}(\beta_{ut}^\gamma \beta_{ut}^{Z*}) \\
 & + GH_9 [\text{Re}(\beta_{ut}^\gamma \eta^{Z*}) - \text{Re}(\beta_{ut}^\gamma \bar{\eta}^{Z*})] + GH_{10} \text{Re}(\beta_{tu}^\gamma \beta_{tu}^{Z*}) + GH_{11} \text{Im}(\beta_{tu}^\gamma \theta) , \quad (13)
 \end{aligned}$$

where F_i , G_i , ... are very lengthy functions of the Mandelstam variables s and t , and of the masses of the particles present. For the interested reader, the authors the full expressions in Mathematica format are available in <http://mars.fis.uc.pt/~plhc-top/public/publications.shtml>. See also [27]. These expressions were obtained with the help of the FeynCalc package [28].

Another interesting calculation that this full set of FCNC operators allows us to do is the contribution to the production of $t\bar{t}$ pairs at the LHC. This arises from the interference of the SM tree-level diagrams and diagrams with *two* anomalous vertices. Thus, the resulting cross sections are, once again, of the order $1/\Lambda^4$. In fact, in [3] we had calculated the interference between the SM processes $q\bar{q} \rightarrow t\bar{t}$ and $gg \rightarrow t\bar{t}$ and the double FCNC diagrams from the strong sector. We now completed the calculation, with the contributions from both the electroweak and the strong sectors as shown in the diagrams of figure (5). As with the cross section for top + jet production, the final expressions are extremely cumbersome and will not be presented here, but are available upon demand. Finally, we did not study the production of top quarks of the same sign, because once again terms of dimension eight in the effective Lagrangian would have to be taken into account for a consistent and complete description.

FIG. 5: Feynman diagrams for FCNC $t\bar{t}$ production.

V. TOP PRODUCTION VIA FCNC INTERACTIONS AT THE TEVATRON AND LHC

With the full cross sections computed, the anomalous operators considered here contribute to the following physical processes: $pp \rightarrow tj$, $pp \rightarrow t\bar{t}$, $pp \rightarrow tZ$, $pp \rightarrow t\gamma$ and $pp \rightarrow th$, where j is a jet and h is the Higgs boson. All these processes were the subject of detailed studies in previous papers. However, this is the first time that both strong and electroweak operators will be used in the analysis of the process $pp \rightarrow tj$. As defined by our criteria in the introduction, the study of the effective FCNC operators with one top quark and at least one gauge boson is now complete.

The cross sections derived here may be applied to any collider we wish to study. In particular, as we will shortly see, the anomalous FCNC interactions here considered would already have a sizeable impact on Tevatron top physics, if the top FCNC branching ratios were large. We are mostly interested in LHC physics, so our philosophy will be to use all available data from the Tevatron experiments to constrain the values of the anomalous couplings. This will enable us to curtail the available parameter space and refine our LHC predictions. As we will see, the Tevatron data has a substantial impact on what one might expect for FCNC single top production at the LHC.

We remind the reader that, for processes of single top production via FCNC, since there are no interferences with the SM [34], our FCNC cross sections constitute *extra* contributions to the SM cross sections. In other words, our anomalous cross sections add to the expected SM values. In table III we present the SM predictions for the single top cross sections at the LHC, against which the size of our FCNC contributions must be compared.

Cross Section	t -channel	s -channel	tW mode
σ_{LHC}^t	$150 \pm 6 \text{ pb}$	$7.8 \pm 0.7 \text{ pb}$	$44 \pm 5 \text{ pb}$
$\sigma_{\text{LHC}}^{\bar{t}}$	$92 \pm 4 \text{ pb}$	$4.3 \pm 0.3 \text{ pb}$	$44 \pm 5 \text{ pb}$

TABLE III: Single top-quark production cross sections predictions for the LHC. The errors include scale uncertainties, parton density function uncertainties, and uncertainties in the top mass. The value $m_t = 171.4 \pm 2.1$ GeV was used. See refs. [29] for details.

A brief summary of our procedures: we generated a large set of complex random values for the anomalous couplings. The range of values chosen for each of the coupling constants was $10^{-12} < |a/\Lambda^2| < 1$, where a stands for a generic coupling and the scale of new physics, Λ , is in TeV. For an excellent discussion on the order of magnitude of the anomalous couplings see [30]. We discard those combinations of values of the couplings for which the several FCNC branching ratios we computed earlier are larger than 10^{-2} . This is a conservative approach, since 10^{-2} is below all experimental upper bounds shown in table I. Only the Tevatron bound on the strong FCNC decay can be smaller, but this is incorporated in the analysis. When an acceptable combination of values is found, we then use it to compute the cross sections for the various processes. All cross sections were obtained by integrating the corresponding partonic cross section with the CTEQ6M partonic density functions [31], with a factorization scale μ_F set equal to m_t . We also imposed a cut of 15 GeV on the p_T of the final state partons.

In figure (6) we plot the FCNC anomalous contribution to the value of the total cross section for $t + \text{jet}$ against the sum of branching ratios of the FCNC decay of the top to a gluon and a u quark plus the decay to a gluon and a c quark. We show the cross section values for the Tevatron, for the LHC at a low operating energy of 10 TeV and for its nominal center-of-mass energy of 14 TeV. This result includes direct top production and the production of a top quark alongside a light quark or a gluon, computed

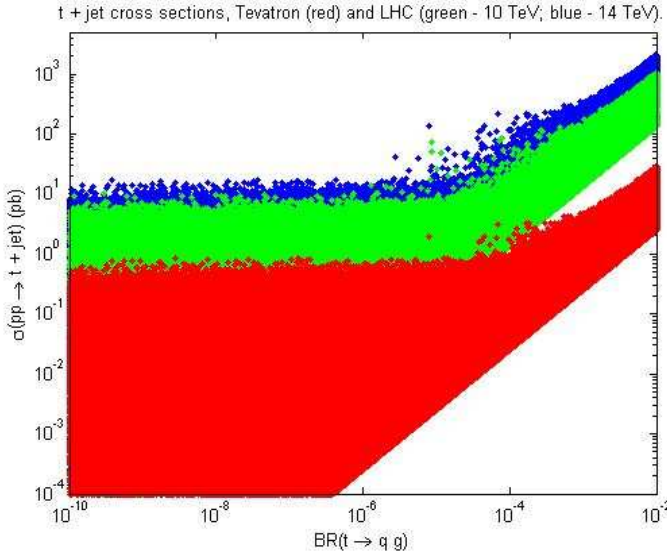


FIG. 6: Total FCNC contributions to the cross section of top + jet production as a function of the sum of the gluon FCNC branching ratios, for the Tevatron (red) and LHC (green - 10 TeV; blue - 14 TeV).

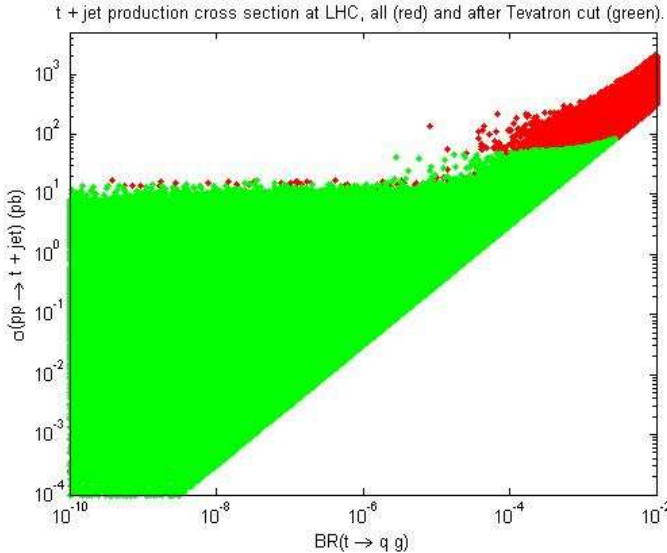


FIG. 7: Total FCNC contributions to the cross section of top + jet production at the LHC as a function of the sum of all strong FCNC branching ratios. The points which survive the Tevatron cut are shown in green.

in [1, 2, 3, 4], as well as the new electroweak sector contributions, that is

$$\begin{aligned} \sigma(pp \rightarrow tj) = & \sigma^S(pp \rightarrow gq \rightarrow t) + \sigma^S(pp \rightarrow gg \rightarrow t\bar{q}) + \sigma^S(pp \rightarrow gq \rightarrow gt) + \\ & \sigma^S(pp \rightarrow q\bar{q} \rightarrow t\bar{q}) + \sigma^{EW}(pp \rightarrow q\bar{q} \rightarrow t\bar{q}) + \sigma^{INT}(pp \rightarrow q\bar{q} \rightarrow t\bar{q}) + \\ & \sigma^S(pp \rightarrow qq \rightarrow tq) + \sigma^{EW}(pp \rightarrow qq \rightarrow tq) + \sigma^{INT}(pp \rightarrow qq \rightarrow tq) , \end{aligned} \quad (14)$$

where the superscript S stands for strong contribution, EW for electroweak and INT for the interference terms between the strong and the electroweak contributions. As is plain to see from fig. (6), the FCNC contributions to single top production can already be quite large at the Tevatron, so the results from that collider need to be taken into account. We emphasize that the same anomalous couplings are used to compute the cross sections at any center of mass energy. There is also little difference between the LHC cross sections at 10 or 14 TeV, though of course the higher energy corresponds to larger values. From

now on all LHC results will correspond to $\sqrt{s} = 14$ TeV.

Let us look more carefully at the LHC predictions, by imposing the existing experimental constraints from the observed cross sections of single top production at the Tevatron: the calculated FCNC contribution to the cross section for single top at the Tevatron was forced to be smaller than the experimental error obtained in the latest single top measurement of the $s+t$ channels, $\sigma_{s+t}^{Tevatron} = 2.2 \pm 0.7$ pbarn [12] (see also [13]). By looking at figure (7), it is clear that the Tevatron constraints make a significant impact on what can be probed at the LHC. With one million points generated, the highest value for the strong branching ratio is found to be around 0.3%. Also, the allowed values for the cross sections drop from a few thousand pbarn to less than 100 pbarn. Nevertheless, the LHC will still be able to further probe this process in the first years of running.

Another very important point worth mentioning is that, even when the strong branching ratio becomes negligible, we still have plenty of points above the 10 pbarn line. In other words, a modification in the electroweak sector related to FCNC top interactions can be sensed in an apparently strong process such as $pp \rightarrow t j$. Note that the largest anomalous FCNC contributions to top plus jet production at the LHC come from processes with gluons in the initial state, and therefore would correspond to an alteration of the strong interaction. A measurement of an excess of a few pbarn in this cross section does not necessarily mean new physics coming from the strong sector - it could mean new physics with its origin in the electroweak sector. An experimental limit in this cross section is automatically translated in a limit for the strong branching ratio. The reverse, however, is not true - an experimental limit in the strong branching ratio will tell us nothing about the cross section of top + jet production, due to the inclusion of the contributions from the electroweak sector.

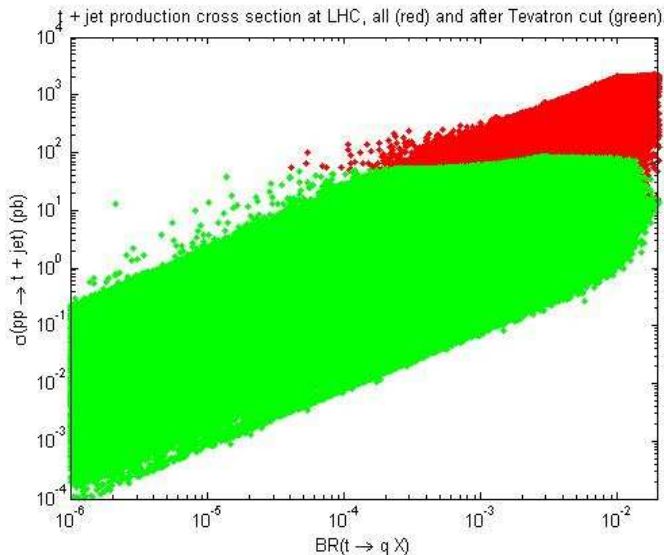


FIG. 8: Total FCNC contributions to the cross section of top + jet production at the LHC as a function of the sum of all FCNC branching ratios (strong and electroweak). The points which survive the Tevatron cut are shown in green.

In figure (8) we again show the extra FCNC contribution to the cross section for top plus jet production in pbarn, but now against the sum of all FCNC branching ratios, that is, $Br(t \rightarrow qg) + Br(t \rightarrow q\gamma) + Br(t \rightarrow qZ)$, where a sum in $q = u, c$ is implicit. With over one million points generated, we found $Br(t \rightarrow qZ) < 1.4\%$ and $Br(t \rightarrow q\gamma) < 1.8\%$ for the electroweak branching ratios, after the Tevatron constraints were imposed. These constraints on the branching ratios are 1-sigma values (68% C.L.). Once again, the total cross section is shown in red, and in green we show the values for the cross section after the constraints from the Tevatron were imposed. Once more we see that the cross section is bound to be below 100 pbarn, and that an experimental bound on the branching ratio can be translated into a bound on the cross section. It is interesting to note that even for a sum of the branching ratios below 10^{-5} , which is well below the sensitivity expected for the LHC, we can still have cross sections of a few pbarn. Therefore, an excess in the total single top cross section has to be interpreted with great care.

In figure (9) we show the FCNC cross section for top plus Z production at the LHC, against the

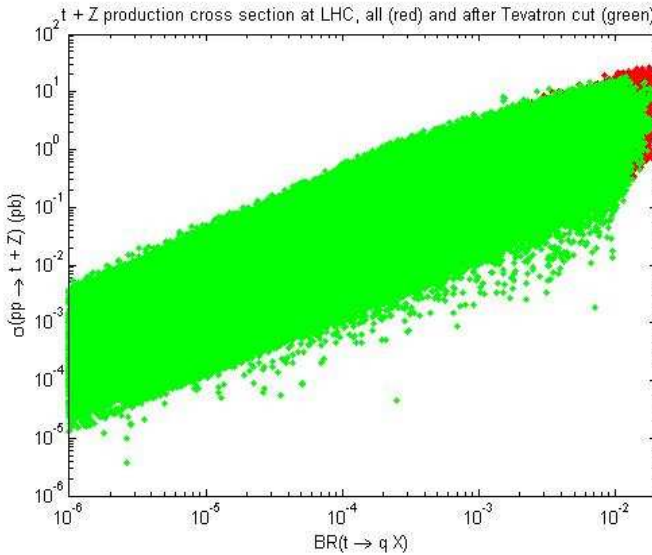


FIG. 9: FCNC cross section for top + Z production at the LHC as a function of the sum of all FCNC branching ratios (strong+electroweak). The points which survive the Tevatron cut are shown in green.

total FCNC branching ratios. As we can see, for this observable the Tevatron cut produces no sizeable exclusion region, and the maximum value of the cross section amounts to about ~ 10 pb. Nevertheless, there is a small region for the larger values of the branching ratio that the Tevatron has managed to exclude. The corresponding plot for the FCNC cross section for $t + \gamma$ production is not shown here, since the constraints from the Tevatron are even milder and have no bearing on the final result. Moreover, the total $t + \gamma$ cross section is found to be even smaller than that for $t + Z$.

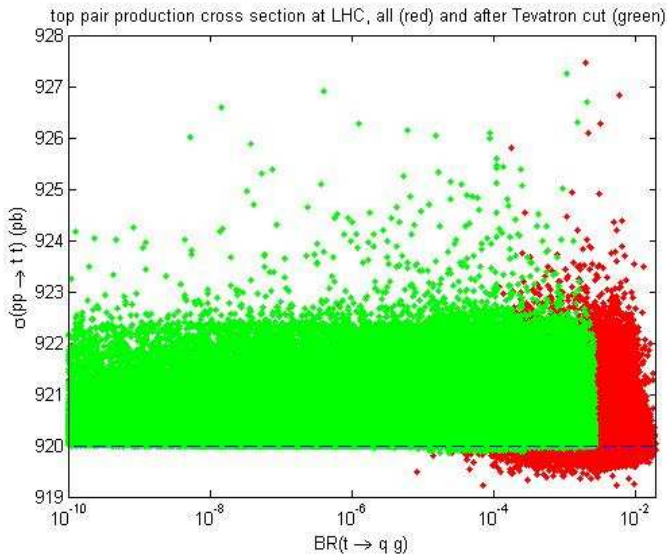


FIG. 10: Total $t\bar{t}$ production cross section at the LHC as a function of the sum of the strong FCNC branching ratios. The dashed line corresponds to the expected SM value, the red points are excluded using Tevatron single-top data.

Finally, in figure (10) we plot the total cross section for $t\bar{t}$ production at the LHC - by “total” we mean including both the SM result and the anomalous FCNC contributions to it. These latter contributions result, as was explained earlier, from interferences between SM diagrams and FCNC ones. It is crucial to verify the impact that our single-top FCNC operators may have on double top production, as a consistency check - if we are changing top quark physics in one given channel, what are the consequences

in others? Thus, the $t\bar{t}$ cross section results already existing could, in principle, be used to constrain single top FCNC operators. However, we have checked that whilst varying the anomalous coupling constants in the range described above, the FCNC extra contribution to the $t\bar{t}$ cross section cannot reach more than 0.64 pbarn at the Tevatron, and 7.3 pbarn at the LHC.

We observe this feature in figure (9), where we used a value of 920 pbarn to the expected SM $t\bar{t}$ cross section at LHC [32]. In red we show the total cross section, while in green we present the cross section after the Tevatron cuts. The central line is the expected SM cross section at the LHC at 14 TeV. It is interesting to note that the Tevatron data seems to eliminate the destructive interference with the FCNC contributions, and the remaining anomalous contributions in the LHC always increase the $t\bar{t}$ cross section, although not by much. It is plain to see from this plot that even the largest values attained for the LHC cross section for $pp \rightarrow t\bar{t}$ will be well below the expected experimental error for this process. Hence, due to the very small values obtained, the $t\bar{t}$ production cross section gives us no information on the set of FCNC single top operators. Only a future and more precise measurement of this cross section will enable us to use the $t\bar{t}$ data to constrain FCNC single top physics. Note, however, that double and single top processes are already related. The constraints on the FCNC branching ratios are obtained from $t\bar{t}$ production with one top decaying to bW and the other to qZ , $q\gamma$ or qg .

VI. CONCLUSIONS

We have performed a general analysis of the impact of dimension six FCNC effective operators on top quark physics. The electroweak contributions presented in this work complete the impact the set of operators chosen might have on channels of single and double top production. The criteria behind that selection are extremely general: that they do not “spoil” the agreement with physics below the TeV scale, and that FCNC is observed in the interactions of the top with gauge bosons. The inclusion of these new contributions allows us to finally compute the full FCNC contributions to an extremely important physical observable: the cross section for single top + jet production. Our results are trivially applied to both the Tevatron and the LHC, and we have shown that our cross sections already predict substantial contributions to Tevatron cross sections. In fact, we used that fact to constrain our allowed space of anomalous constants: by requiring that our predictions for the Tevatron be below the experimental error for top + jet production, we excluded a sizeable portion of parameter space available to be probed at the LHC. Further, this allowed us to set upper bounds on several FCNC branching ratios, which we summarise in table IV, both at the 68% and 95% confidence level. Notice that there is no difference between the bounds obtained for the electroweak FCNC branching ratios. This is due to the fact that,

Branching ratio	Upper bound (68% C.L.)	Upper bound (95% C.L.)
$BR(t \rightarrow qg)$	0.3 %	0.55 %
$BR(t \rightarrow qZ)$	1.34 %	1.34 %
$BR(t \rightarrow q\gamma)$	1.77 %	1.77 %
$BR(t \rightarrow qX)$	2.15 %	2.77 %

TABLE IV: Upper bounds for top quark FCNC branching ratios obtained after imposing the constraints stemming from current Tevatron results. $BR(t \rightarrow qX)$ is the sum of all possible FCNC branching ratios.

as had been already observed regarding figure 9, the Tevatron bounds have little effect on electroweak processes.

Finally, we proved that the FCNC interactions considered had little impact on $t\bar{t}$ production. In fact, this conclusion highlights the importance of the single top channel - top FCNC interactions, if indeed exist, as is predicted by many an extension of the SM, will manifest themselves in single top physics, not top pair production. The single top channel is thus an exquisite place to look for signals of new physics.

The electroweak contributions were first studied in ref. [4] concerning their impact on channels of top + Z or top + photon production. The emphasis on that work was on the possibility of using physical observables to distinguish between strong and electroweak FCNC contributions. In what regards top +

jet cross sections, we may ask whether it is also possible to use these channels to distinguish between the strong and electroweak FCNC contributions. However, notice that the diagrams for top + jet production from the strong sector and from the electroweak sector have exactly the same structure - whereas for top + Z or top + photon production, the diagrams stemming from the strong FCNC interactions had a strong t -channel contribution, and the electroweak ones a strong s -channel component. This difference in structure of both types of diagrams made it possible, through the analysis of the differential cross sections, to, at least in principle, individuate strong and electroweak cross sections. For the top + jet cross sections, however, the differential cross sections for both sectors are similar. As such, we do not expect that this observable could be used to separate electroweak FCNC physics from that of the strong sector.

The cross sections calculated in this paper demonstrate in a clear manner the importance of the single top channels for studies of FCNC physics. In some cases, the best expected experimental limit will probably come from the study of this channel, in particular at the LHC [25]. It should be stressed, however, that the projections obtained in that study must be regarded as a conservative estimate, since only the contribution from the strong direct single top production was taken into account. This is manifestly insufficient as contributions from other channels of single top production are indeed important, as shown in this work. Those channels will change the kinematics of the final state partons, which might have implications on the overall experimental efficiencies, and increase the total cross section several times when compared with the direct production channel alone.

The top FCNC branching ratios can also vary significantly and are related with the total production cross sections. Although several extensions of the SM predict significant enhancements of the branching ratios (which in some realisations can achieve values of the order of 10^{-4}), most of the studies so far were done at particle level, not taking into account the hadronization of the final-state partons, the existence of backgrounds which might mask the FCNC signals or the efficiencies of the detectors at the LHC. Recent estimates from the LHC experiments [33] show that, even when the systematic errors are very much enlarged (for instance, by taking a conservative 5% jet energy resolution value, or by overestimating the contributions from the backgrounds) and with only 1fb^{-1} of data, it will be possible to gain one order of magnitude on the current experimental limits at 95% CL, provided no signal of new physics is found. Assuming this very conservative systematic error, projections can be made for other values of luminosities and/or center-of-mass energies. If the center-of-mass energy for the LHC is changed to only 10 TeV, the total $t\bar{t}$ production cross section changes by roughly a factor 2, which will degrade the current estimates for the 95% limits to $\text{Br}(t \rightarrow qZ) \sim 10^{-2}$ and $\text{Br}(t \rightarrow q\gamma) \sim 10^{-3}$, with only 100 pb^{-1} of luminosity. These limits are still within the interesting experimental probing region.

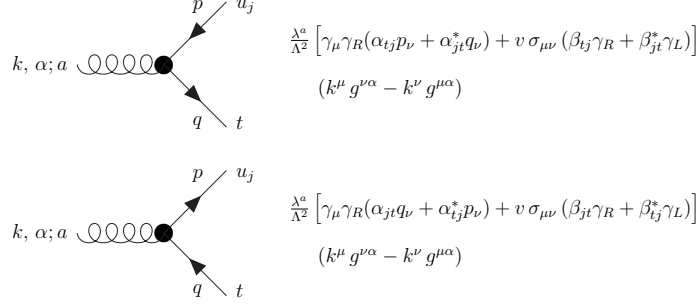
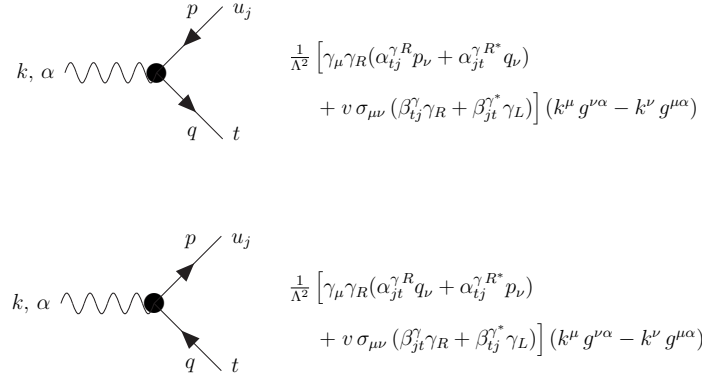
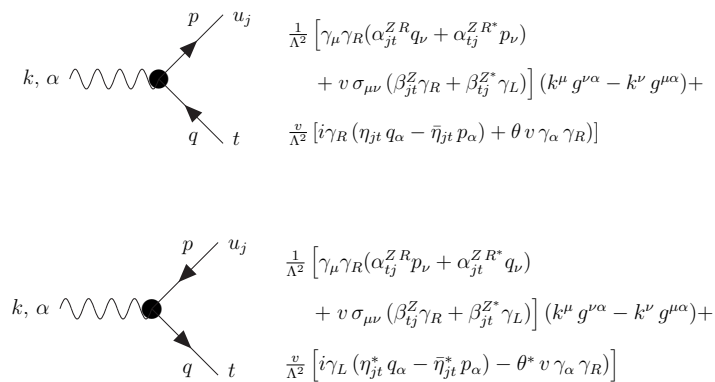
In order to do a complete physics program survey, clearly a new Monte Carlo generator must be developed which will incorporate the contributions from all single top FCNC processes studied so far, the hadronization of all parton level particles and the interface with the simulation programs of the experiments if available. This will be the subject of the next work, whereupon the predictions stemming from cross sections calculated in this paper can be elaborated in realistic detector scenarios.

Acknowledgments: This work is supported by Fundação para a Ciência e Tecnologia under contracts POCI/FP/81950/2007, POCI/FP/81934/2007 and PTDC/FIS/70156/2006. R.G.J. is supported by FCT under contract SFRH/BD/19781/2004. R.S. is supported by the Framework Programme 7 via a Marie Curie Intra European Fellowship, contract number PIEF-GA-2008-221707.

APPENDIX A: FEYNMAN RULES FOR THE FCNC VERTICES

In this appendix we present the Feynman rules for the FCNC vertices used in the calculations. In the strong sector we will only use the Feynman rule with two quarks and one gluon. We show the rules for a t quark entering the vertex and for a t quark leaving the vertex.

-
- [1] P. M. Ferreira, O. Oliveira and R. Santos, Phys. Rev. D **73** (2006) 034011.
 - [2] P. M. Ferreira and R. Santos, Phys. Rev. D **73** (2006) 054025.
 - [3] P. M. Ferreira and R. Santos, Phys. Rev. D **74** (2006) 014006.

FIG. 11: Feynman rules for anomalous $g \bar{u}_i t$ and $g \bar{t} u_i$.FIG. 12: Feynman rules for anomalous $\gamma \bar{u}_i t$ and $\gamma \bar{t} u_i$.FIG. 13: Feynman rules for anomalous $Z \bar{u}_i t$ and $Z \bar{t} u_i$.

- [4] P. M. Ferreira, R. B. Guedes and R. Santos, Phys. Rev. D **77** (2008) 114008.
- [5] W. Buchmüller and D. Wyler, *Nucl. Phys.* **B268** (1986) 621.
- [6] P. J. Fox, Z. Ligeti, M. Papucci, G. Perez and M. D. Schwartz, arXiv:0704.1482 [hep-ph].
- [7] J. Carvalho *et al.*, *Eur. Phys. J.* **C 52** (2007) 999-1019.

- [8] T. Lari *et al.*, Report of Working Group 1 of the CERN Workshop “Flavour in the era of the LHC”, hep-ph/0801.1800.
- [9] CMS Physics TDR: Volume II, CERN/LHCC 2006-021, <http://cmsdoc.cern.ch/cms/cpt/tdr/>.
- [10] F. del Aguila, M. Perez-Victoria and J. Santiago, JHEP **0009** (2000) 011 [arXiv:hep-ph/0007316].
F. del Aguila, M. Perez-Victoria and J. Santiago, Phys. Lett. B **492** (2000) 98 [arXiv:hep-ph/0007160].
- [11] E. Malkawi and T. Tait, *Phys. Rev.* **D54** (1996) 5758;
T. Han, K. Whisnant, B.L. Young and X. Zhang, *Phys. Lett.* **B385** (1996) 311;
T. Han, M. Hosch, K. Whisnant, B.L. Young and X. Zhang, *Phys. Rev.* **D55** (1997) 7241;
K. Whisnant, J.M. Yang, B.L. Young and X. Zhang, *Phys. Rev.* **D56** (1997) 467;
M. Hosch, K. Whisnant and B.L. Young, *Phys. Rev.* **D56** (1997) 5725;
T. Han, M. Hosch, K. Whisnant, B.L. Young and X. Zhang, *Phys. Rev.* **D58** (1998) 073008;
K. Hikasa, K. Whisnant, J.M. Yang and B.L. Young, *Phys. Rev.* **D58** (1998) 114003;
T. Tait and C. P. Yuan, *Phys. Rev.* **D63**, (2001) 014018;
D. O. Carlson, E. Malkawi, and C. P. Yuan, *Phys. Lett.* **B337**, (1994) 145;
T. G. Rizzo, *Phys. Rev.* **D53**, (1996) 6218;
T. Tait and C. P. Yuan, *Phys. Rev.* **D55**, (1997) 7300;
D. Espriu and J. Manzano, *Phys. Rev.* **D65**, (2002) 073005.
B. Grzadkowski, J. F. Gunion and P. Krawczyk, *Phys. Lett.* B **268** (1991) 106.
- [12] CDF Coll., “Combination of CDF Single Top Quark Searches with 2.2 fb^{-1} of Data”, CDF Note 9251. http://www-cdf.fnal.gov/physics/new/top/public_singletop.html
- [13] V. M. Abazov *et al.* [D0 Collaboration], *Phys. Rev. D* **78** (2008) 012005.
- [14] CDF Coll., “Search for top quark production via flavor-changing neutral currents at CDF”, CDF Note 9440. http://www-cdf.fnal.gov/physics/new/top/public_singletop.html
- [15] P. M. Ferreira, R. B. Guedes and R. Santos, *Phys. Rev.* **D75** (2007) 055015.
- [16] J. A. Aguilar-Saavedra, *Acta Phys. Polon. B* **35** (2004) 2695.
- [17] M.E. Luke and M.J. Savage, *Phys. Lett.* **B307** (1993) 387;
D. Atwood, L. Reina and A. Soni, *Phys. Rev.* **D55** (1997) 3156;
J.M. Yang, B.L. Young and X. Zhang, *Phys. Rev.* **D58** (1998) 055001;
J. Guasch and J. Solà, *Nucl. Phys.* **B562** (1999) 3;
D. Delepine and S. Khalil, *Phys. Lett.* **B599** (2004) 62;
J.J. Liu, C.S. Li, L.L. Yang and L.G. Jin, *Phys. Lett.* **B599** (2004) 92;
G. Eilam, M. Frank and I. Turan, *Phys. Rev.* **D74** (2006) 035012;
J. J. Cao, G. Eilam, M. Frank, K. Hikasa, G. L. Liu, I. Turan and J. M. Yang, *Phys. Rev.* **D75** (2007) 075021;
A. Arhrib and W. S. Hou, JHEP **0607** (2006) 009;
A. Arhrib, K. Cheung, C. W. Chiang and T. C. Yuan, *Phys. Rev.* **D73** (2006) 075015;
J. Guasch, W. Hollik, S. Penaranda and J. Sola, *Nucl. Phys. Proc. Suppl.* **157** (2006) 152;
D. Lopez-Val, J. Guasch and J. Sola, hep-ph/0710.0587 ;
J. A. Aguilar-Saavedra, *Phys. Rev.* **D67** (2003) 035003 [Erratum-ibid. **D69** (2004) 099901];
F. del Aguila, J. A. Aguilar-Saavedra and R. Miquel, *Phys. Rev. Lett.* **82** (1999) 1628;
T. P. Cheng and M. Sher, *Phys. Rev.* **D35** (1987) 3484;
S. Bejar, J. Guasch and J. Sola, *Nucl. Phys.* **B600** (2001) 21;
C. S. Li, R. J. Oakes and J. M. Yang, *Phys. Rev.* **D49** (1994) 293 [Erratum-ibid. **D56** (1997) 3156];
G. M. de Divitiis, R. Petronzio and L. Silvestrini, *Nucl. Phys.* **B504** (1997) 45
J. L. Lopez, D. V. Nanopoulos and R. Rangarajan, *Phys. Rev.* **D56** (1997) 3100;
G. Eilam, A. Gemintern, T. Han, J. M. Yang and X. Zhang, *Phys. Lett.* **B510** (2001) 227.
- [18] ALEPH Coll., A. Heister *et al.*, *Phys. Lett.* **B543** (2002) 173;
DELPHI Coll. J. Abdallah *et al.* *Phys. Lett.* **B 590** (2004) 21;
OPAL Coll., G. Abbiendi *et al.*, *Phys. Lett.* **B 521** (2001) 181;
L3 Coll., P. Achard *et al.*, *Phys. Lett.* **B 549** (2002) 290.
- [19] ZEUS Coll., S. Chekanov *et al.*, *Phys. Lett.B* **559** (2003) 153.
- [20] CDF Coll., “Search for the Flavor Changing Neutral Current Decay $t \rightarrow Zq$ in $p\bar{p}$ Collisions at $\sqrt{s} = 1.96 \text{ TeV}$ with 1.9 fb^{-1} of CDF-II Data”, CDF Note 9202, 2008. http://www-cdf.fnal.gov/physics/new/top/2008/tprop/TopFCNC_v1.5/
- [21] CDF Coll., F. Abe *et al.*, *Phys. Rev. Lett.* **80** (1998) 2525.
- [22] M. Beneke *et al.*, “Top quark physics”, in “Standard Model physics (and more) at the LHC”, G. Altarelli and M. L. Mangano eds., Geneva, Switzerland: CERN (2000), [arXiv:hep-ph/0003033].
- [23] A. A. Ashimova and S. R. Slabospitsky, arXiv:hep-ph/0604119. H1 Coll., A. Aktas *et al.*, *Eur. Phys. J.* **C33**, (2004), 9.
- [24] CDF Coll., V. M. Abrazon *et al.* *Phys. Rev. Lett.* **99**, 191802 (2007).
- [25] Teh Lee Cheng, (PhD thesis), University of London, July 2007.
Sensitivity of ATLAS to FCNC single top quark production Cheng, T L; Teixeira-Dias, P ATL-PHYS-PUB-2006-029; ATL-COM-PHYS-2006-056.- Geneva : CERN, Aug 2006.
- [26] F. Larios, R. Martinez and M. A. Perez, *Phys. Rev. D* **72** (2005) 057504;
R. D. Peccei, S. Peris and X. Zhang, *Nucl. Phys. B* **349** (1991) 305;
T. Han, R. D. Peccei and X. Zhang, *Nucl. Phys. B* **454** (1995) 527;

- R. Martinez, M. A. Perez and J. J. Toscano, Phys. Lett. B **340** (1994) 91;
 T. Han, K. Whisnant, B. L. Young and X. Zhang, Phys. Rev. D **55** (1997) 7241.
- [27] M. Won, *Combined effects of strong and electroweak effective FCNC operators in top production at the LHC*, Master's Thesis, University of Coimbra;
 R. B. Guedes, *Flavour Changing at Colliders in the Effective Theory Approach*, PhD Thesis, University of Lisbon.
 Both available in <http://mars.fis.uc.pt/~plhc-top/public/publications.shtml>.
- [28] R. Mertig, M. Bohm and A. Denner, Comput. Phys. Commun. **64** (1991) 345.
- [29] W. Bernreuther, J. Phys. G **35** (2008) 083001 and references therein;
 N. Kidonakis, Phys. Rev. D **74** (2006) 114012;
 N. Kidonakis, Phys. Rev. D **75** (2007) 071501.
- [30] J. Wudka, Int. J. Mod. Phys. A **9** (1994) 2301.
- [31] J. Pumplin *et al.*, JHEP **0207** (2002) 012.
- [32] M. Cacciari, S. Frixione, M. M. Mangano, P. Nason and G. Ridolfi, JHEP **0809** (2008) 127.
- [33] *Top quark properties*, ATLAS note, *in preparation*.
- [34] Or those interferences are exceedingly small, as mentioned regarding the processes 6, 7 and 8 from table II.